Combined Optimal Low-Thrust and Stable-Manifold Trajectories to the Earth–Moon Halo Orbits

G. Mingotti, F. Topputo, and F. Bernelli-Zazzera

Aerospace Engineering Department, Politecnico di Milano, Via La Masa, 34 - 20156, Milano, Italy

Abstract. In this paper we incorporate the low-thrust propulsion in the stable manifold technique to design transfer trajectories to the halo orbits around L_1 and L_2 of the Earth–Moon system. The problem is stated in an optimal control scheme and solved using direct transcription and collocation; the dynamics is discretized over an uniform time grid using a sixth-order linear multi-point method. The resulting transfers are made up by a spiral arc that targets a piece of the stable manifold associated to the final orbit. Thanks to the generality of this approach, halo-to-Moon transfers are also computed combining unstable manifolds and low-thrust. Furthermore, complete Earth-to-Moon transfers via halos can also be constructed. Results show the feasibility of this kind of transfers requiring moderate propellant mass fractions and feasible times of flight.

Keywords: Low-Thrust Trajectory, Optimal Control, Invariant Manifold, Halo Orbits
PACS: 45.50.Pk, 91.10.Sp

INTRODUCTION

The use of halo orbits for future new-concept space missions seems to be unquestionable because their unique features can be exploited to satisfy a large class of mission constraints. In particular, following the original ideas of Farquhar [1], a L_2 libration point satellite can be used to have a real-time communication link between the far side of the Moon and the Earth. By placing another single relay satellite at the cislunar libration point L_1, a point-to-point communication network, covering most of the lunar surface, could be established [2]. Other applications concern the studies of Heppenheimer [3] on the possibility to set a permanent space station at L_2, and those of Broucke [4] and Prado [5] on free-fall trajectories between the libration points and the primaries.

Since the ISEE-3 mission was carried out in 1978 [6], halo orbits have been fully understood and their dynamical properties have been exploited to design the trajectories leading to them. Further improvements in recent years have been obtained by approaching the problem under the perspective of the dynamical system theory [7]. This procedure has allowed the trajectory design for the Genesis mission [8]. The well-established method to design Earth-to-halo transfers can be shortly stated: in order to reach the final orbit at a zero cost, the spacecraft has to be placed on the stable manifold associated to the halo. Once on this manifold, the dynamical system, by itself, provides at bringing the spacecraft to its nominal orbit. To this aim, it is important to check whether or not the stable manifold associated to a certain orbit approaches the Earth. In the Sun–Earth system this happens for a wide class of halos, and so a direct transfer from a low Earth orbit is possible with a single-impulse maneuver. In the Earth–Moon system the stable manifold associated to the halo orbits around L_1 or L_2 *does not* approach the Earth (figure 1). This means that a direct transfer from a LEO is not allowed in the Earth–Moon frame. On the other hand, the unstable manifold of the halos does approach the Moon and so a direct transfer from a halo to a LMO is theoretically possible. Nevertheless, once the low-thrust propulsion is selected, this transfer requires a further spiral arc to circularize the spacecraft around the Moon.

This work deals with the design of transfer trajectories to the halo orbits around L_1 and L_2 in the Earth–Moon system. The idea is to place the spacecraft on a point belonging to the stable manifold, located away from the Earth, by means of a low-thrust spiral arc, solution of an optimal control problem. In this way, the optimal control and the dynamical system theories are merged together to define the whole transfer trajectory; the benefits coming from the use of both the low-thrust propulsion (i.e. high specific impulse) and the ballistic arcs (i.e. zero cost) can be exploited.

The first work facing the combination of a thrust and a n-body ballistic arc was carried out by Belbruno [9] in the context of the LGAS mission. A spiral arc was linked to a transit orbit that led to a ballistic capture at the Moon. This proved the conjecture of Conley [10] on the existence of orbits connecting regions around the Earth and the Moon. Moreover, this work paved the way for the design of the trajectory for the SMART-1 mission [11].

Concerning the low-thrust trajectories for libration point missions, Starchville and Melton computed solutions in

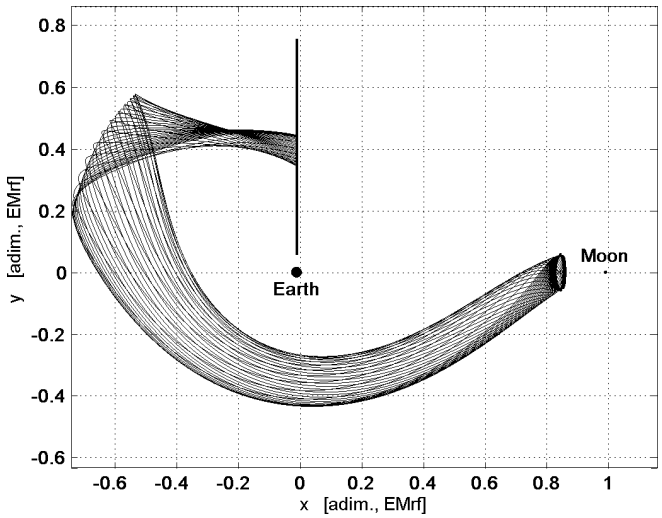

FIGURE 1. Interior branch of the stable manifold associated to a L_1 halo orbit ($A_z = 8000\,\text{km}$) in the Earth–Moon rotating frame. It is clear that the stable manifold, at least in a reasonable time, does not approach the Earth.

both the circular [12] and the elliptical [13] restricted three-body problems. These solutions linked a high altitude Earth orbit with the L_2 point of the Earth–Moon system. Folta and Beckman [14] computed examples of trajectories leaving the Earth with low-thrust spirals and going to the L_2 point of the Sun–Earth system. Lo and Chung [15] implemented the idea of Farquhar in the frame of a lunar sample return mission; nevertheless, this work was based on impulsive maneuvers. Finally, Senent et al [16] studied low-thrust transfers to reach the halo orbits in the Sun–Earth system.

In this work we compute low-thrust transfers from the Earth to the halo orbits around both L_1 and L_2 of the Earth–Moon system. The transfer is stated as an optimal control problem and solved via direct transcription and collocation. The spacecraft is assumed to be initially in a GTO and a low-thrust arc is used to place it, in terms of position and velocity, on the stable manifold associated to the final orbit. The matching condition, which is the final boundary condition of the optimal control problem, is parameterized with two time variables that uniquely define a point on the stable manifold. Thanks to the generality of this approach, halo-to-Moon transfers are also computed by means of unstable manifolds and low-thrust arcs. Hence, a complete Earth-to-Moon transfer via halo orbits can also be constructed. This kind of transfers would be useful in all mission where the release of a payload in a halo orbit before going to the Moon is required.

The remainder of the paper is as follows. In the next section the problem is stated in terms of dynamical system and optimal control problem. The problem is then translated into a NLP optimization and solved. The implemented sixth-order linear multi-point discretization scheme is further illustrated. The last section shows the obtained results in terms of propellant mass fraction and time of flight.

PROBLEM STATEMENT

In this section we briefly illustrate the dynamical system describing the motion of the massless particle in the restricted three-body problem. A detailed derivation of the equations of motion can be found in the classical book of Szebehely [17] or the book of Belbruno [18]. In particular, our description concerns the *controlled* 3D restricted three-body problem. The optimal control problem is presented referring to the book of Bryson and Ho [19].

Dynamics

The differential equations describing the motion of a negligible mass (spacecraft) under the simultaneous gravitational attraction of two primaries (Earth and Moon in this work) can be written in a synodic reference frame

$$\begin{aligned} \ddot{x}-2\dot{y} &= \Omega_x+u_x, \\ \ddot{y}+2\dot{x} &= \Omega_y+u_y, \\ \ddot{z} &= \Omega_z+u_z. \end{aligned} \tag{1}$$

Subscripts denote the partial derivatives of the function

$$\Omega(x,y,z)=\frac{1}{2}(x^2+y^2)+\frac{1-\mu}{r_1}+\frac{\mu}{r_2}+\frac{1}{2}\mu(1-\mu), \tag{2}$$

with respect to the coordinates of the spacecraft (x,y,z). The vector $\mathbf{u}=\{u_x,u_y,u_z\}^T$ denotes instead the control function that is the force per unit mass (i.e. the acceleration) given by the low-thrust engine. System (1) is written in dimensionless units: the sum of the masses of the two primaries, their relative distance, and the angular velocity of the Earth and the Moon on their orbits, are set to one. The fundamental parameter of this formulation is the mass factor μ, which stands for the ratio of the smaller primary mass on the total system mass; in the present study we have assumed $\mu=0.012150\,6683$.

When the motion is purely ballistic ($\mathbf{u}=0$) there is only one constant of motion, the Jacobi integral, associated to the system (1)

$$C(x,y,z,\dot{x},\dot{y},\dot{z})=2\Omega(x,y,z)-(\dot{x}^2+\dot{y}^2+\dot{z}^2)=\text{const.} \tag{3}$$

Equation (3) represents a five-dimensional manifold for the states of the problem within the six-dimensional phase space. Once an initial condition is given, the Jacobi integral defines allowed and forbidden regions for the motion of the spacecraft. The ballistic restricted three-body problem has five equilibria: three collinear points (L_1, L_2, and L_3) are aligned with the primaries; two triangular points (L_4 and L_5) are located at the vertex of two equilateral triangles with the primaries.

Collinear points behave, in a linear analysis, like the product saddle $\times$ center $\times$ center meaning that their neighborhood is characterized by the presence of planar and vertical Lyapunov orbits, three-dimensional halo orbits, quasi-halos, and Lissajous trajectories, all due to the presence of the center parts. Associated to each of these "objects" there are two invariant subspaces, the stable and unstable manifolds, whose presence is due to the saddle part.

Among all these objects, depicting the complete picture of the phase space, this paper is focused on the halo orbits and on their associated invariant manifolds. Halo orbits are computed numerically by solving a two-point boundary value problem [20]. Invariant manifolds can be obtained by flowing, under system (1), the linear subspaces spanned by the stable and unstable eigenvectors of the monodromy matrix associated to the orbit.

Optimal Control Problem

The controlled restricted three-body problem can be written in the first-order form

$$\begin{aligned} \dot{x} &= v_x, \\ \dot{y} &= v_y, \\ \dot{z} &= v_z, \\ \dot{v}_x &= 2v_y+\Omega_x+u_x, \\ \dot{v}_y &= -2v_x+\Omega_y+u_y, \\ \dot{v}_z &= \Omega_z+u_z, \end{aligned} \tag{4}$$

with $v_x=\dot{x}$, $v_y=\dot{y}$, and $v_z=\dot{z}$. In a compact explicit form, system (4) reads

$$\dot{\mathbf{y}}=\mathbf{f}(\mathbf{y}(t),\mathbf{u}(t),\mathbf{p},t), \tag{5}$$

where $\mathbf{f}$ stands for the vector field, $\mathbf{u}=\{u_x,u_y,u_z\}^T$ is the control vector, and $\mathbf{y}=\{x,y,z,v_x,v_y,v_z\}^T$ is the state vector. We note that system (4) degenerates into system (1) when $\mathbf{u}=0$. In addition, the dynamics is also allowed

to incorporate n constant parameters $\mathbf{p} = \{p_1, \ldots, p_n\}^T$ useful for the definition of the optimal control problem. We aim at finding, according to the standard optimal control theory, the control vector history $\mathbf{u} = \mathbf{u}(t)$ that minimizes the following scalar performance index or objective function

$$J = \frac{1}{2} \int_{t_i}^{t_f} \mathbf{u}^T \mathbf{u} \, \mathrm{d}t, \tag{6}$$

while satisfying certain mission constraints. These constraints are represented by two boundary conditions, defined at the end points of the optimal control leg, and by an inequality condition defined along the whole arc.

Initial Boundary Condition

Trajectory optimization problems are usually stated as two-point boundary value problems. The generic initial boundary condition can be formulated as

$$\psi_i \equiv \psi\left[\mathbf{y}(t_i), \mathbf{u}(t_i), \mathbf{p}, t_i\right] = 0. \tag{7}$$

The undertaken strategy dealing with the low-thrust arc is made by two stages: in the first one the spacecraft is propelled tangentially in order to raise its semimajor axis in the minimum time; the optimal control problem is then solved between the tangential spiral and the stable manifold. Hence, the initial state of the optimal control problem, $\mathbf{y}(t_i)$, corresponds to the end-point of the tangential thrust arc starting from the perigee of the initial GTO, namely $\mathbf{y}_0$. The point $\mathbf{y}(t_i)$ depends so on the following two scalars, which will be part of the parameter vector $\mathbf{p}$:

- ω, that is the perigee anomaly of the initial GTO with respect to x-axis of the synodic reference frame, $0 \leq \omega \leq 2\pi$;
- τ_{Lt}, that stands for the time necessary to elevate the spacecraft, starting from the GTO perigee and forward propagated, by means of tangential thrust arc (figure 2), $\tau_{Lt} > 0$.

Let $\varphi_{\mathbf{u}(\tau)}(\mathbf{y}, t_0, t)$ be the flow at time t of system (4) starting from the initial condition $\mathbf{y}$ and integrated with the control law $\mathbf{u} = \mathbf{u}(\tau)$, $t_0 \leq \tau \leq t$. The end-point of the tangential thrust arc can be formalized as

$$\mathbf{y}_{Lt}(\omega, \tau_{Lt}) = \varphi_{\mathbf{u}_0}(\mathbf{y}_0(\omega), 0, \tau_{Lt}), \tag{8}$$

with $\mathbf{u}_0 = \bar{u}\mathbf{v}/\|\mathbf{v}\|$, $\mathbf{v} = \{v_x, v_y, v_z\}^T$, $0 \leq \tau \leq \tau_{Lt}$, and $\bar{u}$ equal to the maximum thrust level (see the next section). Thus, the first point $\mathbf{y}(t_i)$ of the optimal control leg should be such that

$$\psi_i : \mathbf{y}(t_i) - \mathbf{y}_{Lt}(\omega, \tau_{Lt}) = 0. \tag{9}$$

Final Boundary Condition

In analogy with equation (7), the generic final boundary condition can be written as

$$\psi_f \equiv \psi\left[\mathbf{y}(t_f), \mathbf{u}(t_f), \mathbf{p}, t_f\right] = 0. \tag{10}$$

The final point of the low-thrust arc must lie on the stable manifold associated to the nominal halo orbit chosen for the mission. Since the optimal insertion point cannot be determined a priori, it should be parameterized allowing the parameters to be part of the optimization process (i.e. part of the vector $\mathbf{p}$). A point on the stable manifold can be uniquely identified by means of

- τ_h, that is a time variable taken along the orbit, starting from the nominal initial conditions $\mathbf{y}_{h,i}$ necessary to generate the orbit, $\tau_h > 0$. A generic point of the halo orbit can be written as $\mathbf{y}_{p.o.}(\tau_h) = \varphi_{\mathbf{u}=0}(\mathbf{y}_{h,i}, 0, \tau_h)$;
- $\tau_{s.m.}$, a time parameter taken along the stable manifold, $\tau_{s.m.} > 0$. The generic point $\mathbf{y}_{s.m.}(\tau_h, \tau_{s.m.})$ can be computed by the backward integration $\mathbf{y}_{s.m.}(\tau_h, \tau_{s.m.}) = \varphi_{\mathbf{u}=0}(\mathbf{y}_{p.o.}(\tau_h) \pm \varepsilon \mathbf{v}_s, \tau_h, \tau_h - \tau_{s.m.})$, where $\mathbf{v}_s$ is the stable eigenvector of the monodromy matrix calculated at $t = \tau_h$, and ε is a small scalar (figure 3).

Hence, the final boundary condition will read

$$\psi_f : \mathbf{y}_f(t_f) - \mathbf{y}_{s.m.}(\tau_h, \tau_{s.m.}) = 0. \tag{11}$$

It should be noted that the generic halo orbit is also function of the out-of-plane amplitude A_z; this parameter does not take part to the optimization because it is assumed to be fixed by the mission requirements.

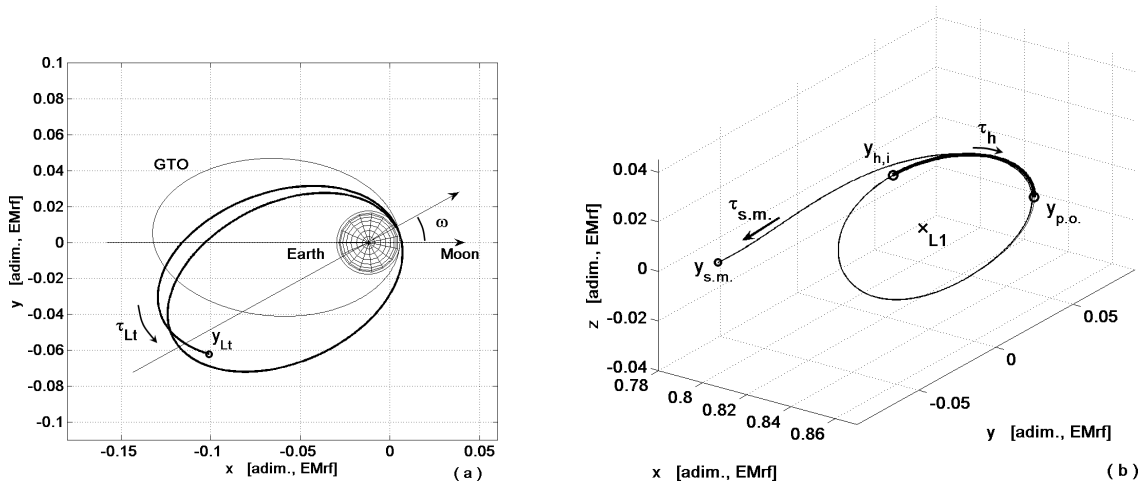

FIGURE 2. Boundary conditions of the optimal low-thrust arc. **(a)**: end point of the tangential thrust spiral $\mathbf{y}_{Lt}$ as a function of ω and τ_{LT}; **(b)**: a generic point $\mathbf{y}_{sm}$ belonging to the stable manifold associated to the final halo and parameterized with τ_h and $\tau_{s.m.}$.

Saturation Condition

When dealing with a low-thrust trajectory optimization problem, the technological features of the engine must be taken into account. In agreement with the current technology, we have assumed the spacecraft equipped with an engine having the following features:

- electric ion propulsion system;
- maximum thrust level $\bar{T}$ equal to 500 mN and 700 mN;
- specific impulse I_{sp} equal to 3000 s.

Among all, the maximum thrust value is the most important condition to consider during the optimization. To this aim, the instantaneous thrust per unit mass at time t, namely T/m, is equal to the acceleration magnitude $\|\mathbf{u}(t)\|$ acting on the spacecraft. This means that the thrust saturation can be easily translated into a nonlinear inequality constraint for the control variable

$$\|\mathbf{u}(t)\| \leq \bar{u}. \tag{12}$$

The maximum acceleration value $\bar{u}$ is obtained considering the maximum thrust level $\bar{T}$ and an initial mass of the spacecraft equal to $m_0 = 1000$ kg.

Once the optimal control problem is solved, the steering law that minimizes the performance index (6) is known as a function of time, namely $\mathbf{u} = \mathbf{u}(t)$, $t \in [t_i, t_f]$. An important characteristic associated to each solution is the *propellant mass fraction*, defined through the rocket equation as

$$f = \frac{m_p}{m_0} = 1 - e^{-\frac{\int_{t_i}^{t_f} \| \mathbf{u}(t) \| \, \mathrm{d}t}{I_{sp}\, g_0}}, \tag{13}$$

where m_p is the propellant mass necessary to carry out the transfer, m_0 is the total mass at launch, and g_0 is the Earth gravitational acceleration at sea level. The fraction f gives an idea about the percentage of propellant mass over the total mass of the spacecraft without considering absolute masses values.

DIRECT TRANSCRIPTION AND COLLOCATION

The basic idea behind the direct transcription method involves discretizing the states and the controls of a continuous trajectory. This technique allows the optimal control problem to be transcribed into a nonlinear programming problem with a finite number of variables and constraints. The idea is to discretize the time domain with a uniform grid

$$t_i = t_1 < t_2 < \ldots < t_N = t_f, \tag{14}$$

where t_i and t_f are respectively the initial and the final time of the optimal trajectory. The N time labels or mesh points define an uniform time grid, according to the formalism proposed by Betts [21]. The nonlinear programming problem variables are mainly made up by the states and the controls evaluated at the grid points, namely $\mathbf{y}_j = \mathbf{y}(t_j)$, $\mathbf{u}_j = \mathbf{u}(t_j)$, $j = 1, \ldots, N$. The whole optimization variable vector has the following structure

$$\mathbf{x} = \{\mathbf{y}_1, \mathbf{u}_1, \mathbf{y}_2, \mathbf{u}_2, \ldots, \mathbf{y}_N, \mathbf{u}_N, \mathbf{p}, t_1, t_N\}^T. \tag{15}$$

We note that the $9N+6$ dimensional vector $\mathbf{x}$ (6 states and 3 controls for each grid point) is further augmented to include the parameters vector $\mathbf{p} = \{\omega, \tau_{Lt}, \tau_h, \tau_{s.m.}\}^T$, described in the previous section, and also the times t_1 and t_N allowing a variable time formulation of the optimal control problem. The basic feature of the collocation method is to replace the original set of ODEs, represented by system (4), with a set of $6(N-1)$ defects $\zeta_j = 0$, imposed at each integration sub-interval $[t_j,\ t_{j+1}]$, $j = 1, \ldots, N-1$. Thus, when including also the 12 two-point boundary conditions (9) and (11), the complete set of $6(N+1)$ nonlinear constraints is

$$\mathbf{c}(\mathbf{x}) = \{\psi_i, \zeta_1, \zeta_2, \ldots, \zeta_{N-1}, \psi_f\}^T. \tag{16}$$

In the same way, the saturation condition can be rewritten in terms of the vector $\mathbf{x}$. The N inequality constraints

$$\mathbf{g}(\mathbf{x}) \leq 0, \tag{17}$$

can be obtained by writing the scalar inequality (12) at each grid point.

One of the advantages of the direct transcription method is that it can be carried out avoiding the explicit derivation of the necessary conditions for the optimality. Such feature makes the method appealing for complicated applications and assures versatility and robustness. Furthermore, this procedure, in contrast to indirect methods, does not need to deal with the Lagrange multipliers, whose lack of physical meaning makes very difficult to find appropriate initial guess solutions.

In summary, the nonlinear programming problem requires finding the $9N+6$ components of the vector $\mathbf{x}$ that solve the following problem

$$\min_{\mathbf{x}} \quad F(\mathbf{x}) \quad \text{subject to} \quad \begin{array}{l} \mathbf{c}(\mathbf{x}) = 0, \\ \mathbf{g}(\mathbf{x}) \leq 0. \end{array} \tag{18}$$

where $F(\mathbf{x})$ is the objective function (6) translated in the formalism of the direct transcription: the integral carried out by numerical quadrature as a function of the controls $\mathbf{u}_j$, $j = 1, \ldots, N$.

Discretization Scheme

In order to well-define the optimization problem, we have to discuss how the defects ζ_j are computed. As mentioned, the dynamics is transcribed into a set of $6(N-1)$ equality constraints whose structure is strongly related to the numerical integration method. The integration scheme chosen in this work is a sixth-order linear multi-point method [20]. It deals with a discretization strategy based on a linear approximation of both sides of the first-order system (4). The discrete approximation is made to enforce the respect of the fundamental theorem of calculus, whose exact fulfillment is reproduced at the level of the discrete equations. The method allows to reach a sixth-order accuracy dealing with a general molecule made up by just four grid points, with the exception of the first and the last integration interval where a special five-point molecule is neded. The method assures in this way an accuracy beyond the first Dahlquist's stability barrier together with a reduced computational burden.

The two different types of computational molecules involve two different kinds of defects. The defect associated to the special five-point molecule, used for the first and the last integration interval, is, for the first molecule,

$$\zeta_1 : \hat{\alpha}_1\mathbf{y}_1 + \hat{\alpha}_2\mathbf{y}_2 + \hat{\alpha}_3\mathbf{y}_3 + \hat{\alpha}_4\mathbf{y}_4 + \hat{\alpha}_5\mathbf{y}_5 - h(\hat{\beta}_1\mathbf{f}_1 + \hat{\beta}_2\mathbf{f}_2 + \hat{\beta}_3\mathbf{f}_3 + \hat{\beta}_4\mathbf{f}_4 + \hat{\beta}_5\mathbf{f}_5) = 0, \tag{19}$$

where $\mathbf{f}_j$ indicates the vector field evaluated at the discretized points: $\mathbf{f}_j = \mathbf{f}(\mathbf{y}_j, \mathbf{u}_j, \mathbf{p}, t_j)$. The generic defect associated to any of the intermediate integration intervals is

$$\zeta_j, j = 2, \ldots, N-2 : \alpha_1\mathbf{y}_{j-1} + \alpha_2\mathbf{y}_j + \alpha_3\mathbf{y}_{j+1} + \alpha_4\mathbf{y}_{j+2} - h(\beta_1\mathbf{f}_{j-1} + \beta_2\mathbf{f}_j + \beta_3\mathbf{f}_{j+1} + \beta_4\mathbf{f}_{j+2}) = 0. \tag{20}$$

The $\hat{\alpha}_j$ and α_j coefficients assure the respect of the fundamental theorem of calculus; the $\hat{\beta}_j$ and β_j coefficients coincide instead with the $O(h^6)$ Gregory quadrature formula parameters [22]. The value of such coefficients can be

found in [20]. It is worth noting that this integration scheme allows to compute analytically the Jacobian of both the equality and inequality constraints, and the gradient of the objective function. These feature speeds-up the solution of the Karush-Kuhn-Tucker necessary conditions [21] for the nonlinear programming.

RESULTS

In this section we present the results obtained for the problem illustrated so far. All the halo orbits have been parameterized with the out-of-plane amplitude A_z that we assume to be fixed a priori by the mission requirements (i.e., A_z is not a parameter to be optimized). Three different kinds of mission have been investigated:

- *Earth-to-halo transfers*: trajectory design from a GTO to a halo orbit around either L_1 or L_2 through low-thrust and stable manifolds;
- *Halo-to-Moon transfers*: trajectory design from a halo orbit to a 100 km high planar circular orbit around the Moon by means of unstable manifolds and low-thrust;
- *Earth-to-Moon transfers via halo*: trajectory design from a GTO to a 100 km high planar circular orbit around the Moon via a transit through a L_1 or a L_2 halo orbit.

Once the optimal control problem is solved, the resulting transfer is verified by numerical integration of the system dynamics adopting an eighth-order Runge-Kutta integrator with absolute and relative tolerances set to 10^{-11}. The integration is carried out taking the first grid point $\mathbf{y}_1$ as initial condition, and making a cubic spline of the controls $\mathbf{u}_j$. This higher order method is useful to evaluate the accuracy of the solutions found, that are obtained with a sixth-order method.

Earth-to-Halo Transfers

Earth-to-halo transfers are designed raising the initial GTO by means of a low-thrust arc that ends, in terms of position and velocity, on a point belonging to the stable manifold associated to the final halo. The GTO has perigee and apogee altitudes equal to $h_p = 400$ km and $h_a = 35864$ km, respectively; the transfer begins when the spacecraft is at the perigee.

Table 1 shows some sample solutions for the transfers from the GTO to an $A_z = 8000$ km halo orbit around L_1 (solutions 1 and 2), and to an $A_z = 16000$ km orbit around L_2 (solutions 3 and 4). The optimal control problem is solved considering both values of the maximum thrust per unit mass assumed to be available: $\bar{u} = 5 \cdot 10^{-4}\,\mathrm{m/s^2}$ and $\bar{u} = 7 \cdot 10^{-4}\,\mathrm{m/s^2}$. A typical transfer trajectory, corresponding to the solution 3, is shown in figure 3. In this example the maximum thrust level is $\bar{u} = 5 \cdot 10^{-4}\,\mathrm{m/s^2}$, the time of flight ($\Delta t$) is 147 days, and the propellant mass fraction, as in all the solutions presented, is slightly less than 9%.

Figure 4 shows the magnitude of the optimal control variable $\mathbf{u} = \mathbf{u}(t)$. Along the first part of the transfer the engine is working at the maximum level of thrust available: the motion consists in a tangential spiral arc aimed at raising the semimajor axis of the Earth-centered orbits in the shortest time possible. It is well known, indeed, that in a regime of motion with constant thrust, the tangential thrust strategy is the one that increases the energy (i.e. the semimajor axis) in the minimum time, involving, in this way, also the minimum propellant mass. After this stage, the optimal control problem is solved respecting the two boundary conditions and the saturation inequality discussed above. The spacecraft is now on the stable manifold associated to the final halo; the dynamical system, by itself, will provide at bringing it to the desired orbit.

TABLE 1. Solutions for the transfer from the GTO to the L_1 and L_2 halos, $I_s p = 3000$ s.

Sol. #	Mission	$\bar{u}\,[\mathrm{m/s^2}]$	m_f/m_0	Δt [days]
1	Earth-L_1 Halo	$5 \cdot 10^{-4}$	0.0887	193.1
2	Earth-L_1 Halo	$7 \cdot 10^{-4}$	0.0892	91.5
3	Earth-L_2-Halo	$5 \cdot 10^{-4}$	0.0894	147.2
4	Earth-L_2-Halo	$7 \cdot 10^{-4}$	0.0895	107.6

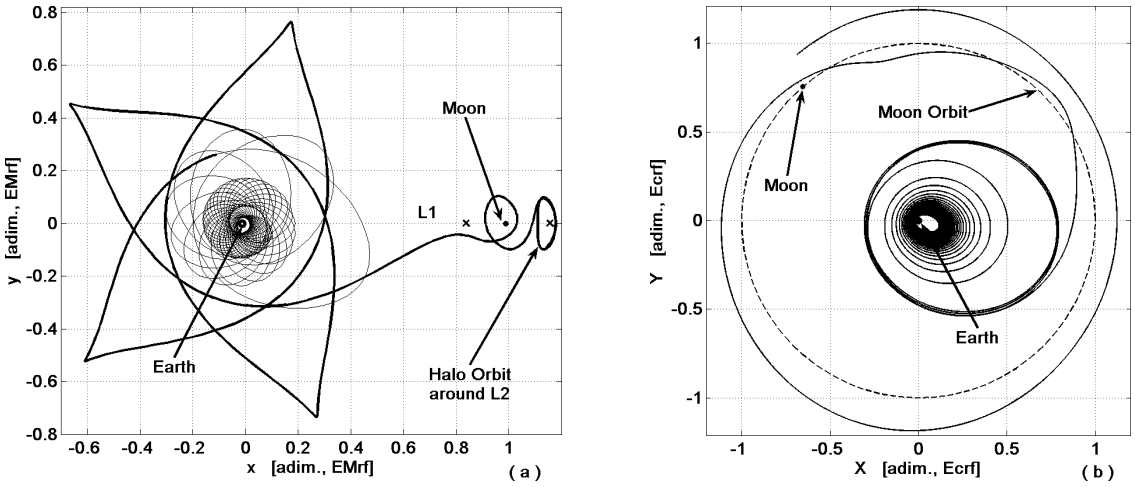

FIGURE 3. Transfer trajectory from the Earth to a L_2 halo orbit corresponding to the solution 3 of table 1. **(a)**: Earth–Moon rotating frame, low-thrust (solid) and stable manifold (bold) arcs; **(b)**: Earth-centered inertial frame, the GTO is raised up to an orbit close to a 5:2 resonance with the Moon where the spacecraft makes its zero cost route to the L_2 halo orbit.

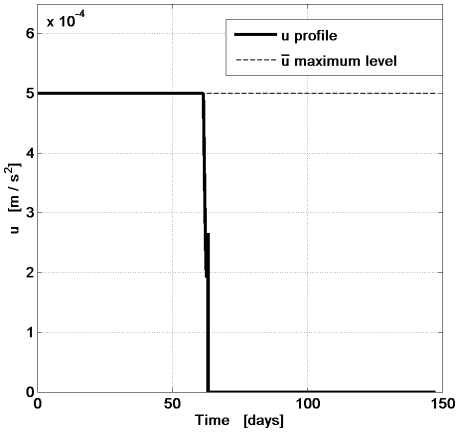

FIGURE 4. Control history profile for the transfer trajectory showed in figure 3.

Halo-to-Moon Transfers

In analogy with the transfer discussed in the previous section, the halo-to-Moon transfers are made up by a piece of unstable manifold, associated to the initial halo orbit, and a low-thrust arc. The optimal insertion point on the thrust arc is again parameterized with two scalars, τ_h and $\tau_{u.m.}$ in this case, and the optimal control problem aims at minimizing the propellant mass as well. The final orbit is a planar circular orbit around the Moon with altitude $h_m = 100\,\text{km}$.

Table 2 shows two sample solutions, one from an $A_z = 8000\,\text{km}$ L_1 halo, and one from an $A_z = 16000\,\text{km}$ L_2 orbit, for this kind of problem. The optimal control problems are solved considering $\overline{u} = 7 \cdot 10^{-4}\,\text{m/s}^2$ as upper bound for the thrust magnitude.

Figure 5 shows the transfer trajectory corresponding the the solution 1 of table 2. The propellant mass fraction is about 4%, and only 32 days are necessary to carry out this transfer. This solution is represented in the Earth–Moon rotating frame where both the ballistic motion - halo and unstable manifold - (bold) and the thrust arc (solid) are clearly visible. In the same figure the magnitude of the optimal control profile is also represented, for the L_1 Halo-Moon transfer. The thrust is first set to zero to allow the spacecraft to fly on the unstable manifold and to get far away from the initial orbit. The thrust is then turned on and the spacecraft is inserted into the optimal thrust arc that brings it to the final planar circular orbit around the Moon.

TABLE 2. Several solutions for the transfer from both the L_1 and L_2 halos to the 100 km altitude orbit around the Moon, $I_sp = 3000$ s.

Sol. #	**Mission**	$\bar{u}$[m/s^2]	m_f/m_0	Δt [days]
1	L_1 Halo-Moon	$7\cdot10^{-4}$	0.0400	32.7
2	L_2 Halo-Moon	$7\cdot10^{-4}$	0.0448	44.4

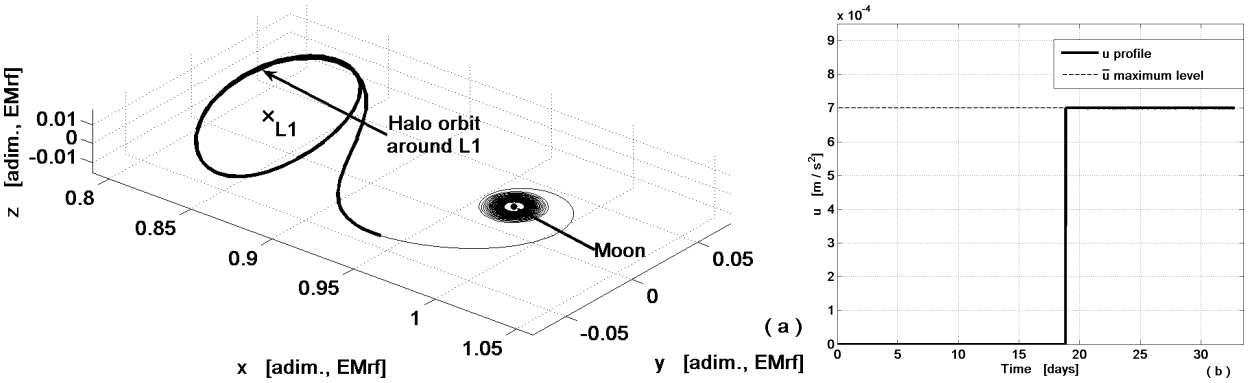

FIGURE 5. Transfer trajectory from a L_1 halo orbit to the Moon corresponding to the solution 1 of table 2. **(a)**: Earth–Moon rotating frame, unstable manifold (bold) and low-thrust arc (solid); **(b)**: control history profile.

Earth-to-Moon Transfers via Halo Orbits

In the previous sections we have described the way to compute low-thrust transfers from the Earth to the halo orbits and from these orbits to the Moon. The developed strategy was aimed at merging together the dynamical system features, arising in the restricted three-body problem, and a thrust arc, solution of an optimal control problem. Now that these two "building blocks" have been developed, a complete Earth-to-Moon transfer can be easily constructed by joining them together. Such kind of transfers would be useful in those missions - as the ones proposed by Farquhar [1]- where it is required first to release a payload in halo orbit and then go to the Moon. The resulting transfers would be like the one originally designed for the LGAS mission [9] that inspired the SMART-1's trajectory [11]. A first spiral arc is necessary to raise the Earth-centered orbit. A ballistic arc, resulting from the simultaneous gravitational attractions of the Earth and the Moon, allows the spacecraft to approach the Moon neighborhood at zero cost. Finally another thrust arc circularizes the spacecraft orbit around the Moon. The main difference between this work and the cited solutions is that the spacecraft is here allowed to orbit, or to release a payload that orbits, one of the two libration points L_1 and L_2.

Two sample solutions are reported in table 3 and are illustrated in figure 6. The two solutions have been obtained assuming the maximum thrust level equal to $\bar{u} = 7\cdot10^{-4}$ m/s^2. The transfer via L_1 requires 124 days and the 12.5% of propellant mass; the one via L_2 lasts 152 days and needs the 13% of propellant.

TABLE 3. Several solutions for the Earth–Moon transfer via halo orbits, $I_sp = 3000$ s.

Sol. #	**Transit Via**	$\bar{u}$[m/s^2]	m_f/m_0	Δt [days]
1	L_1 Halo	$7\cdot10^{-4}$	0.1256	124.2
2	L_2 Halo	$7\cdot10^{-4}$	0.1302	152.5

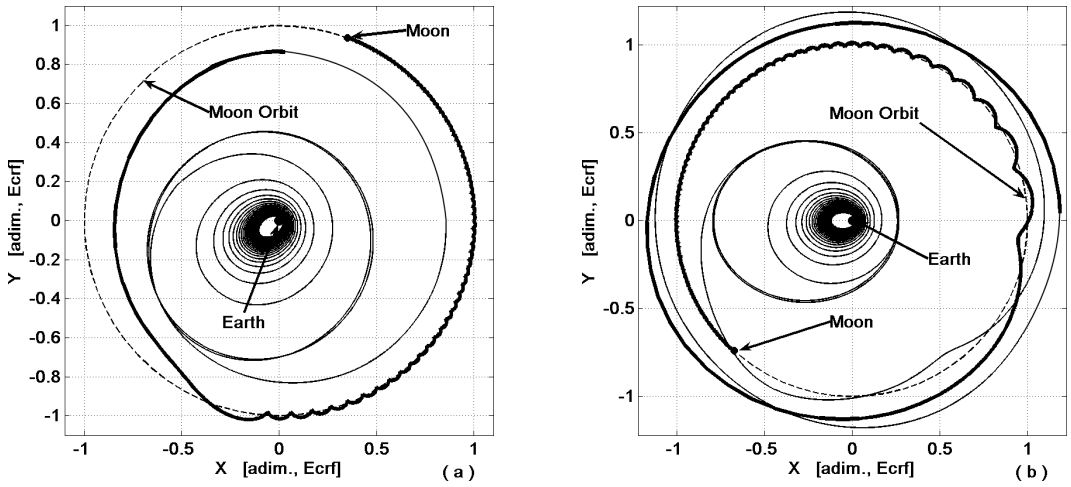

FIGURE 6. Earth–Moon transfers via halo orbits viewed in the Earth-centered frame. **(a)**: Earth–Moon via L_1, Earth-halo (solid) and halo-Moon (bold); **(b)**: Earth–Moon via L_2, Earth-halo (solid) and halo-Moon (bold).

FINAL REMARKS

In this work we have computed trajectories from the Earth to the halo orbits around L_1 and L_2 of the Earth–Moon system, and trajectories from these orbits to the Moon. The basic idea behind the work was to merge together the optimal control and the dynamical system theories to define transfer trajectories taking advantage of both the techniques. In particular the benefits coming from the use of high specific impulse engines and the zero-cost associated to the ballistic arcs have been exploited.

The dynamical system theory deals with the spontaneous motion arising in the restricted three-body problem and represented by the stable and unstable manifolds associated to a certain halo orbit. The optimal control problem is stated in order to minimize the propellant mass associated to the low-thrust arcs. The spirals have been derived in the respect of both the specified boundary conditions and the saturation constraint. The optimal control problem has been solved via a direct transcription and collocation method. The dynamics has been discretized using a sixth-order linear multi-point method that assures a good accuracy while, at the same time, handling a reduced number of grid points. Furthermore, all the solutions have been assessed using a higher-order integration method and a cubic spline interpolation of the control values.

Thanks to the generality of this approach, the whole class of Earth-to-halo, halo-to-Moon, and Earth-to-Moon transfers has been designed. It is remarkable that all the solutions presented require small fractions of propellant mass and reasonable transfer times. In particular, the low-thrust Earth-to-halo transfers represent a brand-new technique that fills a gap in the field of nonlinear astrodynamics.

REFERENCES

1. R. W. Farquhar, *J. Spacecraft Rockets* **4** 1383–1384 (1967)
2. R. W. Farquhar, *Astronaut. Aeronaut.* **10** 59–63 (1972)
3. T. A. Heppenheimer, *J. Spacecraft Rockets* **15** 305–312 (1978)
4. R. Broucke, *J. Guid. Control* **2** 257–263 (1979)
5. B. D. A. Prado, *Acta Astronaut.* **39** 483–486 (1996)
6. R. W. Farquhar, D. P. Muhonen, and D. L. Richardson, *J. Spacecraft Rockets* **14** 170–177 (1977)
7. K. C. Howell, B. T. Barden, and M.W. Lo, *J. Astronaut. Sci.* **45** 161–178 (1997)
8. W. S. Koon, M. W. Lo, J. E. Marsden, and S. D. Ross, "The Genesis Trajectory and Heteroclinic Connections", Paper AAS 99-451, Proc. of AAS/AIAA Astrodyn. Spec. Conf., 1999
9. E. Belbruno, "Lunar Capture Orbits, a Method of Constructing Earth-Moon Trajectories and the Lunar GAS Mission", AIAA Paper no. 97-1054, Proc. of AIAA/DGLR/JSASS Inter. Elec. Propl. Conf., 1987
10. C. C. Conley, *SIAM J. Appl. Math.* **16** 732–746 (1968)
11. J. Schoenmaekers, D. Horas, and J. A. Pulido, "SMART-1: With Solar Electric Propulsion to the Moon", Proc. of the 16th Inter. Symp. on Space Flight Dyn., 2001

12. T. F. Starchville, and R. G. Melton, “Optimal Low-Thrust Trajectories to Earth-Moon L2 Halo Orbits (Circular Problem)”, Paper AAS 97-714, Proc. of AAS/AIAA Astrodyn. Spec. Conf., 1997
13. T.F. Starchville, and R.G. Melton, “Optimal Low-Thrust Transfers to Halo Orbits about the L2 Libration Point in the Earth-Moon System (Elliptical Problem)”, Paper AAS 98-205, Proc. of AAS/AIAA Space Flight Mech. Meeting, 1998
14. D. Folta, and M. Beckman, “Libration Orbit Mission Design: Applications of Numerical and Dynamical Methods”, Proc. of Libr. Point Orbits and Appl., 2002
15. M. W. Lo, and M. J. Chung, “Lunar Sample Return via the Interplanetary Superhighway”, Paper AIAA 2002-4718, Proc. of AIAA/AAS Astrodyn. Spec. Conf., 2002
16. J. Senent, C. Ocampo, and A. Capella, *J. Guid. Control Dynam.* **28** 280–290 (2005)
17. V. Szebehely, *Theory of Orbits: The Restricted Problem of Three Bodies*, Academic Press inc., New York, 1967
18. E. Belbruno, *Capture Dynamics and Chaotic Motions in Celestial Mechanics*, Princeton University Press, Princeton, 2004
19. A. E. Bryson, and Y. C. Ho, *Applied Optimal Control* Wiley, New York, 1975
20. R. Armellin, and F. Topputo, *Celest. Mech. Dyn. Astr.* (to appear)
21. J. T. Betts, *J. Guid. Control Dynam.* **21** 193–207 (1998)
22. J. D. Lambert, *Numerical Methods for Ordinary Differential Systems: The Initial Value Problem*, Whiley, Chichester, 1991